of anisotropic apparent g values, it seems probable that the large number of lines is the result of the superposition of the hydrogen hyperfine splitting spectra of radicals oriented to give different apparent g values. The presence of fewer and broader lines in the spectrum of C_2D_5I than in that of C_2H_5I (Figures 1 and 3) proves that the lines are the result of hyperfine splitting by the hydrogen atoms and is consistent with the effect of deuterium substitution on the simpler ethyl radical spectrum in the glass shown in Figure 2.

Species Responsible for Spectra. Thus far in the discussion the broad spectra have been attributed to spin–orbit coupling with iodine without considering the chemical identity of the species responsible. Iodine species having an unpaired electron which may be present in the γ-irradiated matrices giving these spectra include I, I_2^-, RCHI, RI^+, and RI^-. The first two of these seem to be eliminated by the isotopic substitution results which show that the observed line structure is caused by hyperfine splitting by hydrogen atoms.

One interpretation of the "momentary anneal" effects shown in Figures 4 and 5 is that a process is able to occur at the anneal temperature which converts the species responsible for the complex spectrum to that responsible for the simpler central spectrum. In the case of the polycrystalline ethyl iodide, such a process might be $C_2H_5I^+ + I^-$ (or $C_2H_5I^-$) $\rightarrow C_2H_5$ (or $2C_2H_5$) $+ I_2$, with $C_2H_5I^+$ or $C_2H_5I^-$ being responsible for the broad spectrum. The fact that the "momentary anneal" effect occurs only with crystals frozen after supercooling and does not occur with crystals frozen slowly from a seed, or with those allowed to stand for several days prior to irradiation following freezing, suggests that it is aided by a release of strain energy or change of crystal state that occurs sharply in the narrow temperature range observed for momentary anneal.

It seems more probable that $C_2H_5I^+$ or $C_2H_5I^-$, rather than C_2H_4I, is responsible for the broad spectrum, because the latter offers less possibility for conversion to C_2H_5 during momentary anneal. Esr examination of systems in which C_2H_4I might be formed by the reactions $C_2H_4 + I \rightarrow C_2H_4I$ or $C_2H_3I + H \rightarrow C_2H_4I$, using H and I atoms formed by the photolysis of HI, has shown no evidence of the broad spectra.[11b]

It is probable that the same types of trapped intermediates are formed in the alkyl iodide glasses and in the polycrystalline samples with odd carbon number as in the polycrystalline samples with even carbon number. Thus it appears that a determining factor as to whether a given trapped species produces the broad spectrum is the nature of the crystal lattice in which it resides.

An Electron Diffraction Study of Trimethylsilyl Isothiocyanate and Trimethylsilyl Isocyanate

K. Kimura, K. Katada, and S. H. Bauer

Contribution from the Department of Chemistry, Cornell University, Ithaca, New York. *Received August 25, 1965*

Abstract: The molecular structures of $(CH_3)_3SiNCS$ and $(CH_3)_3SiNCO$ in the gaseous state were determined by electron diffraction using sector–microphotometer data. Neither species was found to have C_{3v} symmetry. The bond distances as observed (center of gravity parameter, r_g) and the bond angles are as follows. For $(CH_3)_3SiNCS$ r_g(C—H) = 1.09 ± 0.02, r_g(C=S) = 1.56 ± 0.01, r_g(N=C) = 1.18 ± 0.01, r_g(Si—N) = 1.78 ± 0.02, r_g(C—Si) = 1.87 ± 0.01 A, and ∠(Si–N–C) = 154 ± 2°. For $(CH_3)_3SiNCO$ r_g(C—H) = 1.10 ± 0.02, r_g(C=O) = 1.18 ± 0.01, r_g(N=C) = 1.20 ± 0.01, r_g(Si—N) = 1.76 ± 0.02, r_g(C—Si) = 1.89 ± 0.01 A, and ∠(Si–N–C) = 150 ± 3°.

Microwave and electron diffraction studies of isocyanates and isothiocyanates have indicated that these molecules do not possess axial symmetry: the valence angles at the nitrogen atom are 128.1 ± 0.5° for HNCO,[1] 130.25 ± 0.25° for HNCS,[2] 132.25 ± 0.25° for DNCS,[2] 125 ± 5° for H_3CNCO,[3] and 142° for H_3CNCS.[4] The more recent microwave studies of H_3CNCS,[5] H_3CNCO,[6] H_3CNSO,[7] and H_3CNCH_2[8] also have shown the presence of internal rotation about a single threefold axis, wherein the barriers to internal rotation of the CH_3 groups are low in both H_3CNCS and H_3CNSO, intermediate in H_3CNSO, and quite high in H_3CNCH_2.

The silanes appear to be different. The infrared and Raman spectra[9] and the microwave spectra[10] of H_3SiNCS and of its deuterated compounds led to the conclusion that these species belong to the symmetry class C_{3v}, with the heavy atoms in linear array. Also,

(1) L. H. Jones, J. N. Shoolery, R. G. Shulman, and D. M. Yost, *J. Chem. Phys.*, **18**, 990 (1950); also studied by electron diffraction by E. H. Eyster, R. H. Gillette, and L. O. Brockway, *J. Am. Chem. Soc.*, **62**, 3236 (1940); and by infrared spectroscopy by C. Reid, *J. Chem. Phys.*, **18**, 1544 (1950).

(2) G. C. Dousmanis, T. M. Sanders, C. H. Townes, and H. J. Zeiger, *ibid.*, **21**, 1416 (1953); also studied by C. Reid, *ibid.*, **18**, 1512 (1950); L. H. Jones and R. M. Badger, *ibid.*, **18**, 1511 (1950); C. I. Beard and B. P. Dailey, *ibid.*, **18**, 1437 (1950).

(3) E. H. Eyster, R. H. Gillette, and L. O. Brockway, *J. Am. Chem. Soc.*, **62**, 3236 (1940).

(4) C. I. Beard and B. P. Dailey, *ibid.*, **71**, 929 (1949).

(5) S. Siegel, Thesis, Harvard University, 1958.

(6) R. F. Curl, Jr., V. M. Rao, K. V. L. N. Sastry, and J. A. Hodgeson, *J. Chem. Phys.*, **39**, 3335 (1963).

(7) V. M. Rao, J. T. Yardley, and R. F. Curl, Jr., *ibid.*, **42**, 284 (1965).

(8) K. V. L. N. Sastry and R. F. Curl, Jr., *ibid.*, **41**, 77 (1964).

(9) E. A. V. Ebsworth, R. Mould, R. Taylor, G. R. Wilkinson, and L. A. Woodward, *Trans. Faraday Soc.*, **58**, 35 (1962).

(10) D. R. Jenkins, R. Kewley, and T. M. Sugden, *ibid.*, **58**, 1284 (1962).

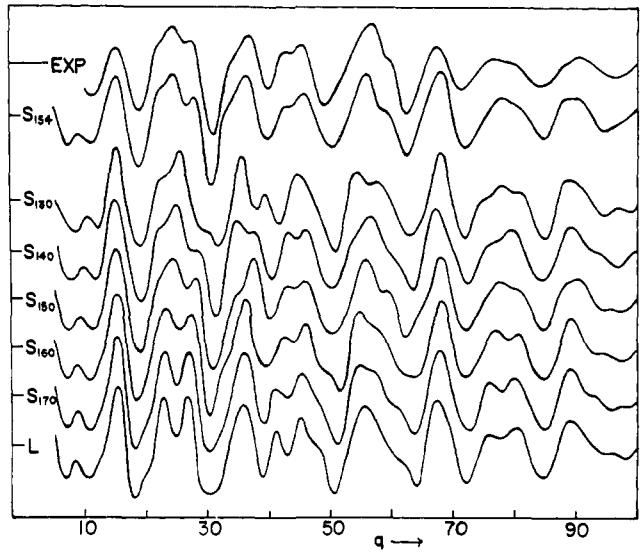

Figure 1. The experimental $M_0(q)$ curve (top) for $(CH_3)_3SiNCS$ compared with the calculated $M_0(q)$ curves for S_{154} (the best model shown in Table I), S_{130} (ϕ = 130°), S_{140} (ϕ = 140°), S_{150} (ϕ = 150°), S_{160} (ϕ = 160°), S_{170} (ϕ = 170°), and L (ϕ = 180°, linear).

Experimental Section

For the diffraction experiments, the samples were purified by vacuum fractionation and checked by mass spectrometric analysis. They were maintained at 1 mm in a 12-l. glass bulb, attached to the nozzle tube. Sectored electron diffraction photographs were taken with the apparatus previously described.[14] Two sectors were used, cut for about 50-kv electrons, to cover a range of q from 10 to 45 A^{-1} [$q = (40/\lambda \sin(\theta/2))$, where λ is the wavelength of the electrons, and θ is the angle of scattering. The stability of the high voltage was carefully checked during each sequence. Also, gold-foil patterns were recorded to provide scale factors. Microphotometer tracings of the diffraction patterns were taken with a Leeds and Northrup microdensitometer. The plates were oscillated about the tracing axis, which passed through the center of the pattern. Optical densities were converted into relative intensities, and the data were reduced in a manner as previously reported.[15]

Analysis and Results

$(CH_3)_3SiNCS$. Figure 1 shows the $M_0(q)$ function which was obtained by combining the experimental total scattered and background intensities, corrected for nonnuclear scattering. Figure 2 is the final radial distribution curve, $f(r)$, computed with a damping factor of μ = 0.0002303 A^2 [see eq 7 in ref 15]. Figure 3 gives the numbering of the atoms and illustrates

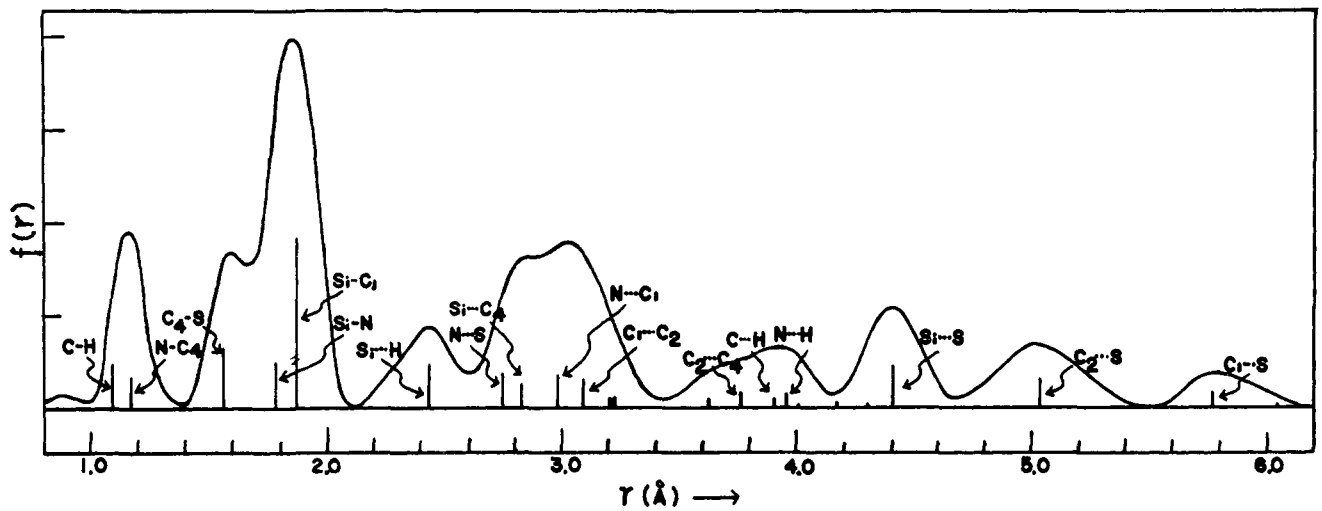

Figure 2. The experimental radial distribution curve for $(CH_3)_3SiNCS$.

the infrared and Raman spectra of $Si(NCO)_4$[11] and $Si(NCS)_4$[12,13] have been interpreted on the basis of T_d symmetry around Si, implying linear structures for the four Si–N–C–O and Si–N–C–S groups, respectively. However, in these and in parallel studies of $(CH_3)_3SiNCO$ and $(CH_3)_3SiNCS$, Goubeau and co-workers[12] concluded that the absence of splitting of the ν_4–ν_6 frequencies does not exclude an angle of 120° or greater at the nitrogen atom.

We considered it important to investigate the molecular structures of these and related compounds. In this paper we report on an electron-diffraction determination of the molecular structures of $(CH_3)_3SiNCS$ and $(CH_3)_3SiNCO$; a second paper will soon follow on three compounds in the class $Cl_nSi(NCO)_{4-n}$.

(11) F. A. Miller and G. L. Carlson, *Spectrochim. Acta*, **17**, 977 (1961).
(12) J. Goubeau, E. Heubach, D. Paulin, and I. Widmaier, *Z. Anorg. Allgem. Chem.*, **300**, 194 (1959).
(13) G. L. Carlson, *Spectrochim. Acta*, **18**, 1529 (1962).

the structure deduced for the compound. In the first step the radial distribution curve was analyzed and a molecular model was deduced using the area criterion. Theoretical intensity curves were then calculated for various models which departed somewhat from that given by the radial distribution curve and compared with the experimental intensity. The radial distribution analysis and the intensity correlations were cycled until the results became self-consistent.

In the final radial distribution curve, the first peak at 1.15 A was resolved with the aid of peak-area counts into two Gaussian peaks at 1.09 and 1.18 A corresponding to bonded C–H and C–N distances. The second peak was assigned to the bonded C–S distance at 1.56 A. The third and strongest peak, at 1.85 A, was resolved into two contributions, the bonded C–Si distance at 1.87 A and the bonded Si–N distance at

(14) J. M. Hastings and S. H. Bauer, *J. Chem. Phys.*, **18**, 13 (1950).
(15) K. Kimura and S. H. Bauer, *ibid.*, **39**, 3172 (1963).

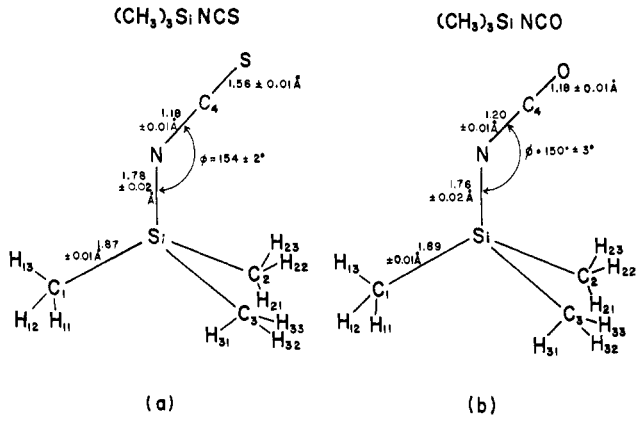

Figure 3. The structures of (a) $(CH_3)_3SiNCS$ and (b) $(CH_3)_3SiNCO$.

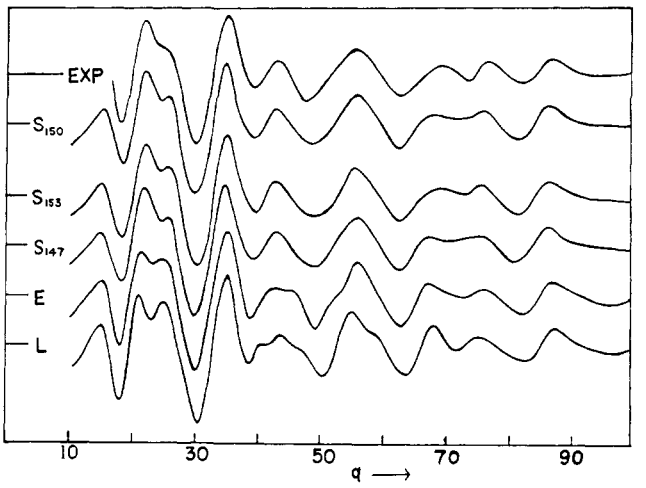

Figure 4. The experimental $M_0(q)$ curve (top) for $(CH_3)_3SiNCO$ compared with the calculated $M_0(q)$ curves for S_{150} (ϕ = 150°, the best model shown in Table I), S_{153} (ϕ = 153°), S_{147} (ϕ = 147°), E(eclipsed, ϕ = 147°), and L (ϕ = 180°, linear).

1.78 A; the latter value was reached at the conclusion of the present analysis. A small peak at 2.44 A was assigned to the nine nonbonded H···Si distances, and the broad curve covering the region of r between 2.6 and 3.4 A may be assigned to the nonbonded N···S, Si···C_4, N···C_1, and C_1···C_2 distances. Here it was reasonably assumed that the N–C–S group was linear. Significant information on the geometry of the molecular skeleton was obtained from the peak at 4.41 A which appeared fairly large, due to the nonbonded Si···S distance, without overlapping with other contributions. A value for ϕ = 154° was obtained for ∠Si–N–C_4. This was the key fact which pointed to the nonlinear structure for SiNCS. It is also supported by three other radial distribution peaks around 3.70, 5.03, and 5.78 A, which may be assigned mainly to the C_2···C_4, C_2···S, and C_1···S distances, respectively, and give 145, 150, and 153° for the Si–N–C_4 angle, respectively. These values for the angle are, however, less reliable than that deduced from the Si···S peak at 4.41 A (154°). Furthermore, the presence of a peak at about 5.03 A indicates that the molecule has a staggered rather than an eclipsed configuration of the NCS group relative to the three Si–Me groups.

The model thus obtained was checked by correlation of intensity curves. A variety of models were tested. Various molecular intensity curves for linear structures (symmetry C_{3v}) with different bond distances were computed and compared with the observed pattern. Ranges of values were selected: 1.72, 1.75, 1.78, 1.81, and 1.84 A for the bonded Si–N distance, with 1.17, 1.19, and 1.21 A for the bonded N–C distance. All the intensity curves computed for the linear models show unacceptable features such as: slight shoulders at q = 12 and 48, instead of the smooth curves which were observed; no shelves at q = 21 and 33 instead of the recorded shelves; and a broad minimum at q = 31 and a small bump at the minimum at q = 62 instead of the simple minima as observed. From theoretical intensities for both staggered and eclipsed configurations with different values of ϕ, it was found that the various configurations showed significant differences in features in the region of q = 20–30. From the systematic comparison of the theoretical intensities with the observed intensity, it was confirmed that the nonlinear (ϕ = 154°), staggered configuration is the best model. The calculated $M_0(q)$ curve for this model (Table I) is given in Figure 1 for comparison with the experimental curve. Also shown are calculated intensities for several models, S_{130}, S_{140}, S_{150}, S_{160}, S_{170}, and L (ϕ = 180°), based on the same parameters but for different values of ϕ. From the intensity correlation, it was found that the best model, S_{154}, has the values $(q_{exptl}/q_{calcd})_{av}$ = 0.9988, σ_q = 0.0058, $[M_{exptl}(q)/M_{calcd}(q)]_{av}$ = 0.98, and σ_M = 0.23. In calculating the

Table I. Structural Parameters for $(CH_3)_3SiNCS$ and $(CH_3)_3SiNCO$

Bond	r_g, A	l_{ij}, A
C—H	1.09 ± 0.02	0.080 ± 0.010
C=S	1.56 ± 0.01	0.040 ± 0.005
N=C	1.18 ± 0.01	0.038 ± 0.005
Si—N	1.78 ± 0.02	0.055 ± 0.005
C—Si	1.87 ± 0.01	0.055 ± 0.005
∠Si–N–C = ϕ = 154 ± 2° staggered		
$(CH_3)_3SiNCO$		
C—H	1.10 ± 0.02	0.065 ± 0.010
C=O	1.18 ± 0.01	0.035 ± 0.005
N=C	1.20 ± 0.01	0.035 ± 0.005
Si—N	1.76 ± 0.02	0.060 ± 0.005
C—Si	1.89 ± 0.01	0.060 ± 0.005
∠Si–N–C = ϕ = 150 ± 3° staggered		

Table II. Mean-Square Amplitudes for $(CH_3)_3SiNCS$ and $(CH_3)_3SiNCO$[a]

	$(CH_3)_3$-SiNCS	$(CH_3)_3$-SiNCO		$(CH_3)_3$-SiNCS	$(CH_3)_3$-SiNCO
C_1–H_{11}	0.080	0.065	H_{21}···C_1	(0.120)	(0.120)
N–C_4	0.038	0.035	H_{23}···C_1	(0.100)	(0.120)
C_4–S	0.040		C_2···C_2	(0.080)	0.080
C_4–O		0.035	C_1···C_4	(0.060)	0.080
C_1–Si	0.055	0.060	C_2···S	(0.085)	
Si–N	0.055	0.060	C_2···O		(0.090)
H_{11}···Si	0.090	0.080	C_1···S	(0.065)	
C_1···N	0.060	0.080	C_1···O		(0.090)
N···S	0.045		Si···C_4	0.055	0.065
N···O		0.037	Si···S	0.075	
C_1···C_2	(0.070)	0.080	Si···O		0.075
H_{12}···N	(0.120)	(0.120)			
H_{11}···N	(0.100)	(0.120)			

[a] Values in parentheses were assumed.

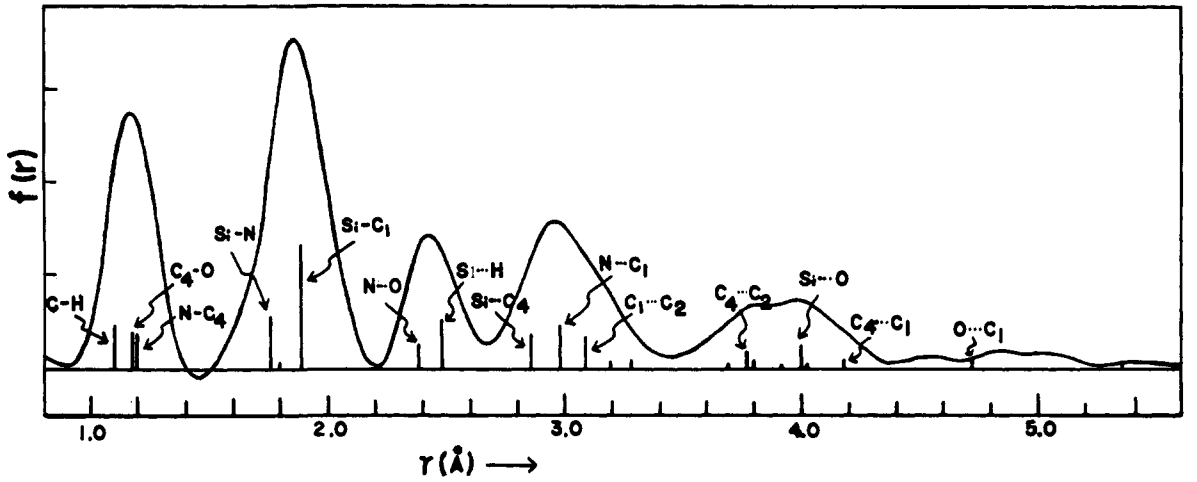

Figure 5. The experimental radial distribution curve for $(CH_3)_3SiNCO$.

theoretical intensity curves the mean-square amplitudes, l_{ij}, listed in Table II were used; some of these were obtained from the present radial distribution analysis and others were assumed.

$(CH_3)_3SiNCO$. The experimental $M_0(q)$ and $f(r)$ curves derived by the same procedures as described above for $(CH_3)_3SiNCS$ are shown in Figures 4 and 5, respectively. The configuration of atoms in $(CH_3)_3$-SiNCO is not so readily deduced as in $(CH_3)_3SiNCS$ because of the lower scattering power of oxygen compared to that of sulfur. However, both the analysis of the radial distribution curve and a comparison of calculated intensities with the experimental one support a similar nonlinear, staggered model for $(CH_3)_3SiNCO$.

The first three peaks in $f(r)$ may be assigned to interatomic distances which are not dependent on a shape of the molecular skeleton, while the fourth peak at 3 A and the doublet near 4 A are due to distances which determine the molecular geometry. The composite features of the fourth peak cannot be accounted for on the assumption of a linear model based on the interatomic distances deduced from the first three peaks. Also the inner peak of the doublet (~3.8 A) does not fit either the linear or the eclipsed models. Features beyond 4.2 A were not considered.

Intensity curves were calculated for a range of models; various combinations of bond distances and bond angles were tested. Some of these are shown in Figure 4. In general, it appears that linear and eclipsed models do not reproduce the intensity function in the region of q from 40 to 50 A^{-1}. The most probable value for the bond angle, ϕ = ∠Si–N–C, was established from consideration of values of the scale factor $(q_{exptl}/q_{calcd})_{av}$, the index of resolution $[M_{exptl}(q)/M_{calcd}(q)]_{av}$, and their standard deviations, σ_q and σ_M, where q in the preceding refers to q values of intensity maxima and minima. The best model, S_{150}, has the values of $(q_{exptl}/q_{calcd})_{av}$ = 1.0012, σ_q = 0.0090, $[M_{exptl}(q)/M_{calcd}(q)]_{av}$ = 0.98, and σ_M = 0.21.[16] The structure parameters of the best model are tabulated in Table I and shown in Figure 3. The mean amplitudes used for the intensity calculations are listed in Table II. The structure parameters for the two compounds agree with one another to within the limits of error.

(16) If the interatomic distances of model S_{150} were multiplied by the value $(q_{exptl}/q_{calcd})_{av}$ = 1.0012 the resultant values of scale factor and its standard deviation would be 1.0002 and 0.0076, respectively.

Discussion

Among the various structures which we considered briefly and discarded without detailed analysis was one in which the Si–N bond distance was lengthened, its axis tilted from the threefold symmetry axis, and the angle at the nitrogen atom reduced so that the longer distances remained in agreement with the well-resolved outer radial distribution peaks. Such a structure implies the presence of a three-minimum potential function for locating the NCS (or NCO) group relative to the CH_3 groups. For the associated wagging motion, the barrier height should be low and the root-mean-square fluctuations in the corresponding nonbonded distances high. There was no indication of such a smearing effect in the experimental radial distribution curves.

The present electron diffraction study has led to closely similar structures for trimethylsilyl isocyanate and the thioisocyanate. The Si–N–CX atoms are not collinear, with ∠Si–N–CS = 154° and ∠Si–N–CO = 150°. Thus, the electron diffraction data indicate structures which were not expected by analogy based on the microwave study of H_3SiNCS,[6] there being substantial differences in the Si–N bond distances and in the ∠SiNC angles. Table III is a summary of reported structural parameters in various isocyanates and isothiocyanates. The bond angle at the nitrogen is less than 180° in all cases except $Si(NCO)_4$, $Si(NCS)_4$, and H_3SiNCS. The compounds $(CH_3)_3SiNCS$ and $(CH_3)_3SiNCO$, along with the others, have short N–C bond distances (1.18 and 1.20 A, respectively). This may be taken as an indication of signifiant contributions by the triple-bonded Lewis resonance structures

$$Si—N=C=S \longleftrightarrow Si—\overset{+}{N}\equiv C—\overset{-}{S}$$

$$Si—N=C=O \longleftrightarrow Si—\overset{+}{N}\equiv C—\overset{-}{O}$$

Silicon–nitrogen bond distances show an unexpected variability. The sum of the covalent radii (Pauling[17]) is 1.87 A; in $N(SiH_3)_3$ the bond distance is 1.738 A,[18] whereas in the silyl isocyanates and thioisocyanates they range from 1.78 and 1.76 A, as reported in this

(17) L. Pauling, "The Nature of Chemical Bond" Cornell University Press, Ithaca, N. Y., 1960, p 246.

(18) K. Hedberg, *J. Am. Chem. Soc.*, 77, 6491 (1955).

Table III. A Summary of Bond Distances and Bond Angles (ϕ) in Isocyanates and Isothiocyanates

	Bond distance, A						
	Si—N	C—N	N=C	C=O	C=S	ϕ, deg.	Ref
HNCO			1.207 ± 0.01	1.171 ± 0.01		128.1 ± 0.5	1
HNCS			1.216 ± 0.002		1.561 ± 0.002	130.25 ± 0.25	2
DNCS			1.216 ± 0.002		1.561 ± 0.002	132.25 ± 0.25	2
H_3CNCO		1.47 (assumed)	1.19 ± 0.03	1.18 ± 0.03		125° ± 5	3
H_3CNCS		1.47	1.22		1.56	142	4
H_3SiNCS	1.714 ± 0.010		1.211 ± 0.010		1.560 (assumed)	180	10
$(CH_3)_3SiNCO$	1.76 ± 0.02		1.20 ± 0.01	1.18 ± 0.01		150 ± 3°	*a*
$(CH_3)_3SiNCS$	1.78 ± 0.02		1.18 ± 0.01		1.56 ± 0.01	154 ± 2	*a*
$Si(NCO)_4$ }						180	12, 13
$Si(NCS)_4$ }							

[a] Present work.

paper, to 1.714 A in H_3SiNCS, to approximately 1.65 A in the $Cl_nSi(NCO)_{4-n}$ sequence.[19] The sensitivity of the Si–N bond distance to the nature of the groups attached to the silicon strongly argues for the assumption that the Si–N bond is more complex than σ^2 derived from an (sp^3) hybrid. The length of the bond appears to increase with increasing electron release by the substituent groups. In turn, the types of orbitals which determine the Si–N bond affect the Si–N–C bond angle. Ebsworth,[20] in summarizing the chemical and some of the physical properties of silylamines, calls attention to the apparent multiple-bond character of Si–N linkages.

Acknowledgments. K. Kimura wishes to thank Professor Y. Morino of Tokyo University for helpful discussions. This work was supported in part by grants from: Office of Naval Research [Contract Nonr-401(41)], and Materials Science Center (Advanced Research Projects Agency). Samples of the two compounds studied were generously given to us by Professor G. S. Forbes and were prepared as described by Forbes and Anderson.[21]

(19) Manuscript in preparation.
(20) E. A. V. Ebsworth, "Volatile Silicon Compounds," The MacMillan Co., New York, N. Y., 1963, Chapter 5.
(21) G. S. Forbes and H. H. Anderson, *J. Am. Chem. Soc.*, **70**, 1222 (1948), and previous publications. For a tabular summary of physical constants, refer to T. Moeller, "Inorganic Chemistry," John Wiley and Sons, Inc., New York, N. Y., 1952, p 476 ff.

Structures of C_7H_{10} Valence Tautomers as Determined by Electron Diffraction

Joseph F. Chiang and S. H. Bauer

Contribution from the Department of Chemistry, Cornell University, Ithaca, New York. *Received September 16, 1965*

Abstract: The structures of the valence tautomers 1,3-cycloheptadiene and Δ^6-bicyclo[3.2.0]heptene have been investigated in the gaseous phase by electron diffraction. Both molecules possess C_s symmetry. In 1,3-cycloheptadiene all but one of the carbon atoms are coplanar; the C atom at the apex is tilted 73° up from the plane. Δ^6-Bicyclo[3.2.0]heptene is in a chair conformation. For the best models the bond lengths and the bond angles are as follows. For 1,3-cycloheptadiene the bond lengths (A) are C_1=C_2 = 1.35, C_2—C_3 = 1.48, C_1—C_7 = 1.54, C_6—C_7 = 1.55, C_1—H_1 = 1.09, and C_7—H_7 = 1.11; $\angle C_3C_2C_1$ = 129° and $\angle C_1C_7C_6$ = 119°. For Δ^6-bicyclo[3.2.0]-heptene C=C = 1.34, C—C = 1.56, C—H = 1.10 A; $\angle C_7C_1C_2$ = 105.5°, $\angle C_1C_2C_3$ = 86.7°, $\angle C_5C_1C_2$ = 109.5°, $\angle C_2C_3C_4$ = 112.9°, $\angle C_6C_7C_1$ = 94.0°, and $\angle C_7C_1C_5$ = 86.0°.

The valence tautomers 1,3-cycloheptadiene and Δ^6-bicyclo[3.2.0]heptene possess unexpected structural features. 1,3-Cycloheptadiene was first synthesized in 1901 by Willstatter.[1] Since then there have been many investigations of this compound. Friess[2] reported that it absorbs in the ultraviolet at λ_{max} = 248 mμ, with log ϵ = 3.87, independent of the solvent used. This was confirmed by Hafner and Rellensmann,[3] who found that in *n*-hexane, λ_{max} = 247.4 mμ, log ϵ = 3.90. The spectrum shows a single broad band which is characteristic of conjugated cyclic dienes.[4-6] Raman spectra of 1,3-cycloheptadiene[7] were interpreted in terms of a *cis* configuration about the double bond in the ring.

(1) v. R. Willstatter, *Ann.*, **317**, 2041 (1901).
(2) P. Pesch and S. L. Friess, *J. Am. Chem. Soc.*, **72**, 5756 (1950).
(3) K. Hafner and W. Rellensmann, *Ber.*, **95**, 2567 (1962).
(4) C. B. Allsopp, *Proc. Roy. Soc.* (London), **A143**, 618 (1939).
(5) V. Henn and L. W. Pickett, *J. Chem. Phys.*, **7**, 439 (1939).
(6) A. C. Cope and L. L. Estes, *J. Am. Chem. Soc.*, **72**, 1129 (1950).
(7) E. V. Sobolev, V. T. Aleksanyan, E. M. Milvitskaya, and M. A. Pryanishnikova, *J. Struct. Chem.* (USSR), **4**, 169 (1963).